# Local atomic and electronic structures of epitaxial strained LaCoO_{3} thin films

G. E. Sterbinsky, P. J. Ryan, J.-W. Kim, E. Karapetrova, J. X. Ma, J. Shi, and J. C. Woicik

Phys. Rev. B **85**, 020403 — Published 11 January 2012

DOI: 10.1103/PhysRevB.85.020403

# Local Atomic and Electronic Structures of Epitaxial Strained $LaCoO_3$ Thin Films

G. E. Sterbinsky,[1,*] P. J. Ryan,[2] J.-W. Kim,[2] E. Karapetrova,[2] J. X. Ma,[3] J. Shi,[3] and J. C. Woicik[1]

[1] *National Institute of Standards and Technology, Gaithersburg, MD 20899, USA*
[2] *Advanced Photon Source, Argonne National Laboratory, Argonne, IL 60439, USA*
[3] *Department of Physics, University of California, Riverside, California 92521, USA*

(Dated: December 5, 2011)

We have examined the atomic and electronic structures of perovskite lanthanum cobaltite ($LaCoO_3$) thin films using Co $K$-edge x-ray absorption fine structure (XAFS) spectroscopy. Extended XAFS (EXAFS) demonstrates that a large difference between in-plane and out-of-plane Co-O bond lengths results from tetragonal distortion in highly strained films. The structural distortions are strongly coupled to the hybridization between atomic orbitals of the Co and O atoms, as shown by x-ray absorption near edge spectroscopy (XANES). Our results indicate that increased hybridization is not the cause of ferromagnetism in strained $LaCoO_3$ films. Instead, we suggest that the strain-induced distortions of the oxygen octahedra increase the population of $e_g$ electrons and concurrently depopulate $t_{2g}$ electrons beyond a stabilization threshold for ferromagnetic order.

Discoveries of novel properties in transition metal (TM) oxides, such as superconductivity in cuprates[1] and colossal magnetoresistance in manganites,[2] have prompted a flurry of research on these materials and proposals for numerous oxide thin film based electronic devices.[3,4] Fabrication of complex oxides in the form of thin films is crucial to the development of such devices. However, when synthesized as a thin film, the properties of a material can differ substantially from those of their bulk counterpart as a consequence of epitaxial strain. A striking example is the appearance of ferromagnetism in strained $LaCoO_3$ (LCO),[5–12] a perovskite oxide that lacks long-range magnetic order in bulk form. Below 100 K, LCO exists in a nonmagnetic insulating state, where the six valence electrons of $Co^{3+}$ occupy the $t_{2g}$ levels of the crystal field split $3d$ states. The $t_{2g}^6e_g^0$ configuration of $Co^{3+}$ is commonly referred to as the low spin (LS) state. Above 100 K, LCO becomes paramagnetic and semiconducting. Upon heating to 500 K, a transition to a paramagnetic and metallic phase occurs. These phase transitions are believed to coincide with spin state transitions of $Co^{3+}$ ions to $t_{2g}^5e_g^1$ intermediate spin (IS) or $t_{2g}^4e_g^2$ high spin (HS) states. However, the exact nature of the spin states present in LCO is not fully understood.[13]

The spin states of the perovskite cobaltites are strongly influenced by competition between the crystal field splitting ($\Delta_{CF}$) of the Co($3d$) states into $e_g$ and $t_{2g}$ levels, which favors a LS configuration, and Hund exchange, which favors a HS configuration. The effects of chemical and hydrostatic pressure on the nonmagnetic to paramagnetic transition temperature illustrate the sensitivity of the spin state to the $e_g$-$t_{2g}$ gap ($\Delta$), where $\Delta = \Delta_{CF} - W/2$, and $W$ is the overlap between Co($3d$) derived $e_g$ and O($2p$) orbitals.[14,15] The dependence of the orbital overlap and crystal field splitting on the Co-O distance ($r_{Co-O}$) and the Co-O-Co angle ($\theta$) are approximated by the expressions $W \propto r_{Co-O}^{-3.5}\sin(\theta/2)$ and $\Delta_{CF} \propto r_{Co-O}^{-5}$.[6,14] Therefore, $\Delta$ can be reduced by an increase in $r_{Co-O}$ or $\theta$. In the case of chemical pressure, replacing lanthanum with a rare earth ion having a smaller ionic radius reduces $\theta$. This increases $\Delta$ and thereby raises the nonmagnetic to paramagnetic transition temperature.[13–15] On the other hand, application of external pressure can induce a transition to the LS state by reducing $r_{Co-O}$ and therefore increasing $\Delta$.[14]

Numerous studies have demonstrated that epitaxial LCO thin films have a ferromagnetic ground state with a Curie temperature near 85 K.[5–12] These works indicate that tetragonal distortion of LCO is critical to the appearance of ferromagnetism, a conclusion supported by theoretical studies.[16] However, the local atomic structure resulting from tetragonal distortion is unclear. Local structure is strongly correlated with magnetic properties, and therefore without knowledge of the local structure the nature of ferromagnetism cannot be well understood.

Previous extended x-ray absorption fine structure (EXAFS) studies of LCO thin films deposited on $(LaAlO_3)_{0.3}(Sr_2AlTaO_6)_{0.7}$ indicate that all six Co-O bonds are of equal length.[17] This result supports the conclusion that ferromagnetic order in LCO is due to strain induced suppression of the Jahn-Teller distortion that has been suggested to occur in bulk LCO.[5] However, existence of a Jahn-Teller distortion in bulk LCO has been called into question by recent studies.[18,19] Furthermore, in other TM perovskite oxide thin films, epitaxial strain causes significant distortion of oxygen octahedra and can also alter octahedral rotations.[20–23] In addition to affecting the spin state as discussed above, distortion and rotation of oxygen octahedra can alter magnetic properties by changing the magnetic exchange energy, which increases with additional overlap between Co($3d$) derived $e_g$ and O($2p$) orbitals, $W$. In this way, strain induced changes in Co-O hybridization can modify the magnetic properties of ferromagnetic perovskite oxides.[20,23] Increased Co-O hybridization has also been posited as a requirement for ferromagnetic ordering in LCO.[6]

In order to provide insight into the nature of ferromagnetism in epitaxial LCO, we have undertaken a detailed investigation of the local and electronic structures of LCO thin films. Bulk LCO has a rhombohedral structure belonging to space group $R\bar{3}c$ with a pseudocubic lattice parameter ($a_0$) of 3.830 Å.[24] The present study examines $\sim$ 20 nm thick LCO films pulsed-laser deposited on $SrTiO_3$ (STO), $a_0 = 3.905$ Å, and $LaAlO_3$ (LAO), $a_0 = 3.791$ Å, substrates for direct comparison.[7] The films are capped with two unit cells of STO. Further details of the deposition and properties of these films can be found in Refs. 7 and 8. STO and LAO substrates have respective lattice misfits of 2.0 % and −1.0 % with LCO. However, while the LCO film deposited on STO is coherently strained, having an in-plane lattice parameter ($a_f$) equal to that of the substrate, the film deposited on LAO is not, having $a_f$ equal to 3.842 Å, presumably due to the increased misfit between LCO and LAO at the growth temperature.[8,25] Thermal stress that occurs upon cooling from the growth temperature has a substantial impact on lattice parameters of LCO thin films.[6] The out-of-plane lattice parameters ($c_f$) of LCO films deposited on STO and LAO substrates are 3.781 Å and 3.864 Å, respectively.[7,8] Lattice parameters were measured by x-ray diffraction at beamlines 6-ID-C and 33-BM-C of the Advanced Photon Source (APS). The different strain states that result from the two substrates have been shown to strongly affect the magnetic properties of LCO, with films deposited on STO being ferromagnetic and films deposited on LAO showing magnetic behavior consistent with that of a spin glass.[7] Thus, differences in the local and electronic structures of these two films reveal aspects of the material that likely determine the magnetic state of LCO.

Co $K$-edge x-ray absorption fine structure (XAFS) spectroscopy was performed at the National Institute of Standards and Technology (NIST) beamline X23A2 of the National Synchrotron Light Source (NSLS) in order to examine the local atomic and electronic structures of the LCO films. A four-element silicon drift detector was used for collection of EXAFS data, while the near edge portion of the XAFS spectrum was measured using a single-element

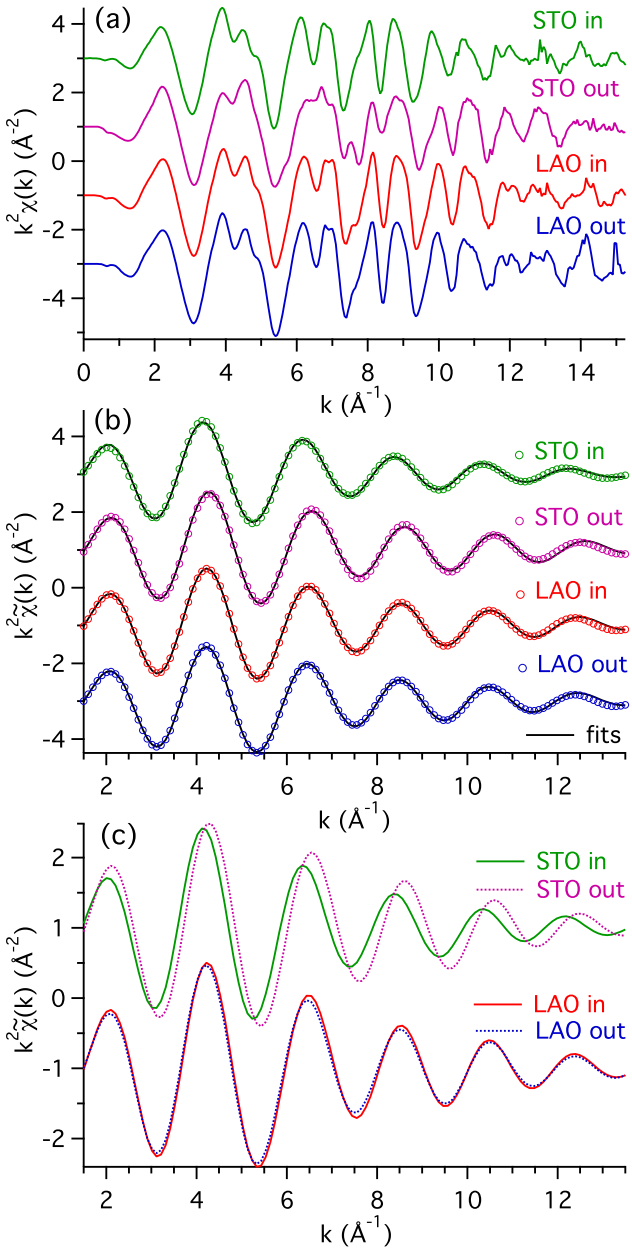


FIG. 1. In-plane and out-of-plane (a) Co $K$-edge EXAFS spectra ($k^2\chi(k)$), and (b, c) Fourier filtered first shell contributions to the EXAFS ($k^2\tilde{\chi}(k)$) of LCO films on STO and LAO substrates. In (b), fits to $k^2\tilde{\chi}(k)$ using the phase and amplitude functions from the LCO powder are also shown. Note the definitive structural changes in the film on STO as compared to the film on LAO, seen in (c).

silicon drift detector inserted into a low temperature cryostat.[26] During the collection of EXAFS data, the films were spun about the surface normal to avoid inclusion of Bragg peaks in the spectra. To account for structural changes resulting from epitaxial strain, EXAFS spectra ($\chi(k)$) were collected with the polarization vector $\hat{\boldsymbol{\varepsilon}}$ of the incident radiation oriented parallel to the film surface and 2° from the surface normal. Because $\chi(k)$ is proportional to $|\hat{\boldsymbol{\varepsilon}} \cdot \hat{\mathbf{r}}|^2$, bonds in the direction of the x-ray polarization vector are preferentially sampled by XAFS. Therefore, in-plane and out-of-plane bond lengths can be separately determined from the polarization dependent data.

To extract the Co-O bond lengths from the EXAFS, each $k^2\chi(k)$ shown in Fig. 1a was Fourier filtered to obtain the contribution to the EXAFS from Co-O single scattering ($k^2\tilde{\chi}(k)$), shown in Figs. 1b and c.[20,27] Each $k^2\tilde{\chi}(k)$ was then fit with the phase and amplitude functions from $k^2\tilde{\chi}(k)$ of a LCO powder, which was measured in transmission.[28] The resulting fits are shown in Fig. 1b. The difference between the in-plane and out-of-plane Co-O bond lengths ($\Delta r_{Co-O}$)

was determined by fitting the in-plane $k^2\tilde{\chi}(k)$ with the phase and amplitude functions from the out-of-plane $k^2\tilde{\chi}(k)$, for each film.

The in-plane and out-of-plane Co-O bond lengths ($r_{Co-O_\parallel}$ and $r_{Co-O_\perp}$, respectively) of LCO deposited on LAO are 1.937 ± 0.004 Å and 1.942 ± 0.004 Å, respectively.[29] These values are slightly larger than the bulk value of $r_{Co-O}$, which is 1.934 Å. The in-plane, out-of-plane, and average Co-O-Co bond angles ($\theta_\parallel$, $\theta_\perp$, and $\theta_{avg}$, respectively) calculated from $r_{Co-O_\parallel}$, $r_{Co-O_\perp}$, $a_f$, and $c_f$ are 165°, 168°, and 166°, respectively. The average Co-O bond length ($r_{Co-O_{avg}}$) is 1.939 ± 0.004 Å, and $\Delta r_{Co-O}$ is −0.005 ± 0.004 Å, indicative of a small distortion of the oxygen octahedra. The small distortion is evident from the subtle difference in the phases of the in-plane and out-of-plane $k^2\tilde{\chi}(k)$, seen in Fig. 1c. On the other hand, a large phase shift is seen between the in-plane and out-of-plane $k^2\tilde{\chi}(k)$ for the film on STO, which makes evident a considerable distortion of the oxygen octahedra. With respect to bulk LCO, $r_{Co-O_\parallel}$ is substantially elongated, having a value of 1.964 ± 0.006 Å, while $r_{Co-O_\perp}$ is contracted to 1.922 ± 0.005 Å. The Co-O-Co bond angles $\theta_\parallel$ and $\theta_\perp$ are 168° and 159°, respectively. This gives a value of 165° for $\theta_{avg}$, which is close to the bulk value of 164°. Values of 1.950 ± 0.006 Å and 0.043 ± 0.008 Å were determined for $r_{Co-O_{avg}}$ and $\Delta r_{Co-O}$, respectively. The values clearly demonstrate that a large strain induced Jahn-Teller like tetragonal distortion of the oxygen octahedra is present in the LCO film deposited on STO.

The effects of the structural distortions on the electronic structure of LCO were probed by Co $K$-edge x-ray absorption near edge spectroscopy (XANES), shown in Fig. 2. For comparison, Ti $K$-edge XANES measured from the STO substrate is also shown. The energy scales in the figure have been aligned with respect to the electron binding energies ($E_0$) of Co and Ti metal, which were taken as the first maximum of the first derivative of the $K$-edge spectra of Co and Ti metal foils. In STO, the energy difference between $E_0$ and the beginning of the pre-edge is larger than in LCO because the formal 4+ charge state of Ti in STO is larger than the formal 3+ charge state of Co in LCO and because of different electron-hole screening in the two materials. The peaks in the STO XANES at 4968.6 eV and 4970.8 eV result from transitions of 1$s$ electrons to 3$d$ derived $t_{2g}$ and $e_g$ levels, respectively.[30] Two distinct peaks are also observed in the LCO pre-edge region at 7709.2 eV and 7711.5 eV. Early studies attributed these features to transitions of 1$s$ electrons to $t_{2g}$ and $e_g$ states, as observed in STO.[31,32] However, more recent charge-transfer multiplet calculations indicate that while the lowest energy pre-edge feature, at about 7709.2 eV, results from 1$s$ to 3$d$ quadrupolar electron transitions, the second feature, at 7711.5 eV, is due to dipolar transitions of 1$s$ electrons to states arising from O(2$p$) mediated intersite hybridization between Co(4$p$) and Co(3$d$) orbitals, i.e., intersite hybridized Co(4$p$)-O(2$p$)-Co'(3d) states, where Co' refers to the next neighbor Co ion.[33] This latter interpretation of the pre-edge features is supported by the angular dependence of the XANES data shown in Fig. 2a, which confirms the respective quadrupolar and dipolar natures of the transitions. When the x-ray polarization vector ($\hat{\boldsymbol{\varepsilon}}$) and wavevector ($\hat{\mathbf{k}}$) are oriented along ⟨100⟩ directions, the intensity of the peak at 7709.2 eV is substantially smaller than when $\hat{\boldsymbol{\varepsilon}}$ and $\hat{\mathbf{k}}$ are along ⟨110⟩ directions. This behavior is consistent with that of the STO $e_g$ peak and demonstrates that this feature also results from quadropolar transitions to $e_g$ levels. On the other hand, the intensity of the peak at 7711.5 eV, $p$-$d$ feature, is invariant with respect to the directions of $\hat{\boldsymbol{\varepsilon}}$ and $\hat{\mathbf{k}}$, which indicates that this pre-edge feature results from dipolar transitions.[33,34]

The intensity of the Co $K$-edge feature at 7711.5 eV is larger in materials with shorter Co-O bonds and larger Co-O-Co bond angles, and is therefore sensitive to overlap between atomic orbitals on the different atomic sites.[33] This feature is more intense for the film deposited on LAO than for the film on STO, measured with the x-ray polarization vector in either the in-plane or out-of-plane direction, as seen in Fig. 2b. The relative intensities therefore indicate stronger hybridization in the film on LAO and weaker hybridization in the film on STO. The weaker hybridization in the film on STO is attributed to the larger average Co-O bond length in the film.

The temperature dependence of Co $K$-edge XANES of the LCO films was also examined. The intensities of the $e_g$ and $p$-$d$ features are independent of temperature between 15 K and 300 K. This result differs from studies of bulk LCO, where the intensity of the $p$-$d$ feature is found to increase upon cooling from room temperature to 15 K.[31] The change in intensity is the result of increased orbital hybridization as the lattice contracts upon cooling. The lattice contraction resulting from cooling of bulk LCO is prevented in LCO films because of adhesion to the STO and LAO substrates, which have thermal expansion coefficients that are approximately half of that of LCO.[6] Thus substantial changes in the pre-edge intensity are not observed upon cooling.

The measured characteristics of the local and electronic structures of the LCO films allow assessment of the factors contributing to ferromagnetism in the films. Co $K$-edge XANES demonstrates that additional hybridization between the Co and O ions, which would increase the electron hopping amplitude and therefore the exchange energy, is not an important parameter for stabilization of ferromagnetism. On the other hand, hole doping is known to introduce ferromagnetism in LCO, where the magnetic state depends strongly on hole concentration. In $La_xSr_{1-x}CoO_3$, a critical concentration of 20% Sr is needed to stabilize ferromagnetism, which results from percolation of ferromagnetic clusters that remain isolated at lower Sr doping levels.[35,36] A critical concentration of HS or IS $Co^{3+}$ might also be sufficient for stabilization of ferromagnetism in LCO. In fact, evidence for a larger population of HS $Co^{3+}$ in the LCO

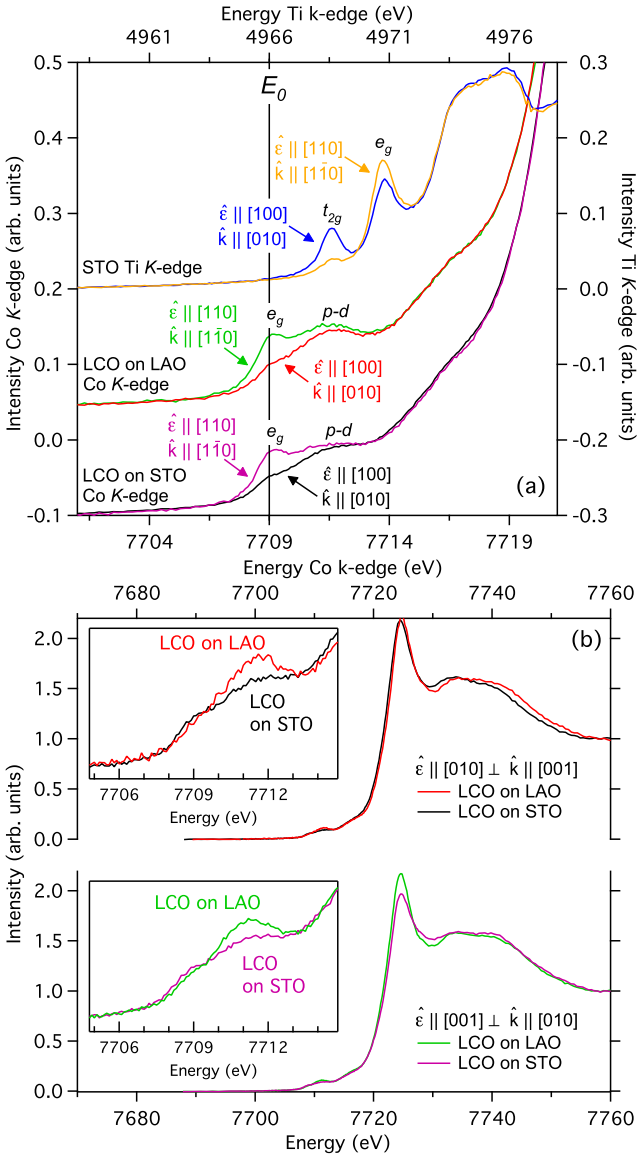


FIG. 2. (a) Co and Ti $K$-edge XANES of LCO films and the STO substrate measured with the x-ray wavevector and polarization vector in-plane along ⟨100⟩ and ⟨110⟩ directions at room temperature. The vertical line shows the position of the electron binding energy ($E_0$). (b) Co $K$-edge XANES of LCO films measured with the x-ray wavevector (polarization vector) along the [010] in-plane direction and the polarization vector (wavevector) along the [001] out-of-plane direction at 15 K. Note the reduced intensity of the hybridization feature in the film on STO, seen in the inset plots.

film deposited on STO with respect to the film on LAO is found in the Co $L_2$-edge x-ray absorption spectroscopy (XAS) presented in Ref. 7. In the film on STO, the maxima of the $L_2$-edge is shifted to slightly higher energy and the shoulder on the high energy side of the peak is reduced in intensity with respect to those of the film on LAO. These changes are consistent with an increase in the number HS $Co^{3+}$ and are observed in bulk LCO as temperature and the population of $e_g$ electrons increases.[19,37,38] In addition, Co $L$-edge XAS studies have demonstrated that the concentration of HS $Co^{3+}$ ions in strained LCO films is considerably higher than in bulk LCO below the ferromagnetic Curie temperature of the films.[37] Like the Co $K$-edge XANES discussed above, the Co $L$-edge XAS spectrum and, therefore, the concentration of HS $Co^{3+}$ remain constant with temperature, which implies that the substrate prevents structural changes that inhibit ferromagnetism in bulk LCO.[37]

The increased population of $e_g$ electrons is a direct result of the structural distortions induced by epitaxial strain. The larger average Co-O bond length of the film on STO will result in a smaller crystal field splitting of the Co($3d$) levels. Furthermore, the Jahn-Teller like tetragonal distortion of the oxygen octahedra in the film on STO will lift the degeneracy of the $e_g$ and $t_{2g}$ levels such that the $d_{x^2-y^2}$ level will shift to lower energy and the $d_{yz}$ and $d_{zx}$ levels

will increase in energy. This will also decrease $\Delta$, which lowers the energy cost of occupation of $e_g$ levels as favored by Hund exchange and results in a relatively large population of $e_g$ electrons in the film on STO. This effect is also observed when hydrostatic pressure is applied to LCO.[14] A pressure induced reduction in $r_{Co-O}$ increases $\Delta$ and causes a transition to the LS state. The structural distortions in the LCO film on LAO also act to reduce $\Delta$. In the film on LAO, the oxygen octahedra are tetragonally distorted and $r_{Co-O_{avg}}$ is larger than that of bulk LCO, although neither the tetragonal distortion nor $r_{Co-O_{avg}}$ are as large as those found in the film on STO. The increase in the Co-O-Co bond angle will also contribute to a smaller $\Delta$. These structural distortions are not sufficient to reduce $\Delta$ to the degree observed in STO. This results in a number of IS or HS $Co^{3+}$ ions insufficient to stabilize ferromagnetism. Instead the IS or HS $Co^{3+}$ ions form isolated ferromagnetic clusters leading to spin glass behavior, as is observed at low hole doping levels in $La_xSr_{1-x}CoO_3$.[35,36,39] In the film on STO, the smaller gap between $e_g$ and $t_{2g}$ levels stabilizes a number of IS or HS $Co^{3+}$ ions sufficient for percolation of ferromagnetic clusters. We note that we cannot directly determine whether HS or IS $Co^{3+}$ is present in the films. An IS state could be stabilized by the tetragonal distortion of the oxygen octahedra, which lifts the degeneracy of the $e_g$ and $t_{2g}$ levels. However, even in the case where the $e_g$ levels are split, a HS state could be favored due to overlap of the $e_g$ bands, as has been suggested previously for LCO thin films.[5] This picture is consistent with Co $L$-edge XAS studies, which find only LS and HS $Co^{3+}$ in LCO films deposited on STO.[38] Furthermore, magnetic moments reduced with respect to those expected from the number of HS $Co^{3+}$ ions also provide support for the presence of ferromagnetic clusters in LCO.[38]

Finally, we note that previous studies have concluded that unbending of Co-O-Co bonds can also stabilize ferromagnetism in LCO.[6,40] However, because increased Co-O-Co bond angles reduce the gap between $e_g$ and $t_{2g}$ levels and increase the hybridization between Co($3d$) and O($2p$) states, the factor influencing ferromagnetism was ambiguous. From the XAFS studies presented herein, we can conclude that enhanced hybridization between ions is not responsible for ferromagnetism in LCO films. Instead, the important parameter for stabilization of ferromagnetism is the concentration of HS or IS $Co^{3+}$, and any structural change that would reduce $\Delta$ can potentially induce ferromagnetism in LCO. In that case, a sufficiently large reduction in the gap between the $e_g$ and $t_{2g}$ derived levels increases the number of IS or HS $Co^{3+}$ above a threshold level at which percolation of ferromagnetic clusters occurs.

The authors thank J. M. Rondinelli and J. W. Freeland for helpful discussions. Use of the NSLS, Brookhaven National Laboratory was supported by the U.S. Department of Energy (DOE), Office of Science, Office of Basic Energy Sciences, under Contract No. DE-AC02-98CH10886. Use of the APS, an Office of Science User Facility operated for the U.S. DOE Office of Science by Argonne National Laboratory, was supported by the U.S. DOE under Contract No. DE-AC02-06CH11357. Additional support from NIST is also acknowledged. G. E. Sterbinsky acknowledges support as a National Research Council Research Associate at NIST. J. X. Ma and J. Shi are supported by DMEA/CNN H94003-10-2-1004.3.

* gsterbinsky@bnl.gov


[1] E. G. Maksimov, Phys. Usp., **43**, 965 (2000).
[2] Y. Tokura and Y. Tomioka, J. Magn. Magn. Mater., **200**, 1 (1999).
[3] R. Ramesh and D. G. Schlom, MRS Bull., **33**, 1006 (2008).
[4] J. Heber, Nature, **459**, 28 (2009).
[5] D. Fuchs, C. Pinta, T. Schwarz, P. Schweiss, P. Nagel, S. Schuppler, R. Schneider, M. Merz, G. Roth, and H. v. Löhneysen, Phys. Rev. B, **75**, 144402 (2007).
[6] D. Fuchs, E. Arac, C. Pinta, S. Schuppler, R. Schneider, and H. v. Löhneysen, Phys. Rev. B, **77**, 014434 (2008).
[7] J. W. Freeland, J. X. Ma, and J. Shi, Appl. Phys. Lett., **93**, 212501 (2008).
[8] S. Park, P. Ryan, E. Karapetrova, J. W. Kim, J. X. Ma, J. Shi, J. W. Freeland, and W. Wu, Appl. Phys. Lett., **95**, 072508 (2009).
[9] A. Herklotz, A. D. Rata, L. Schultz, and K. Dörr, Phys. Rev. B, **79**, 092409 (2009).
[10] A. D. Rata, A. Herklotz, L. Schultz, and K. Dörr, Eur. Phys. J. B, **76**, 215 (2010).
[11] V. V. Mehta, M. Liberati, F. J. Wong, R. V. Chopdekar, E. Arenholz, and Y. Suzuki, J. Appl. Phys., **105**, 07E503 (2009).
[12] R. F. Klie, T. Yuan, M. Tanase, G. Yang, and Q. Ramasse, Appl. Phys. Lett., **96**, 082510 (2010).
[13] N. B. Ivanova, S. G. Ovchinnikov, M. M. Korshunov, I. M. Eremin, and N. V. Kazak, Phys. Usp., **52**, 789 (2009).
[14] J.-S. Zhou, J.-Q. Yan, and J. B. Goodenough, Phys. Rev. B, **71**, 220103 (2005).
[15] M. Tachibana, T. Yoshida, H. Kawaji, T. Atake, and E. Takayama-Muromachi, Phys. Rev. B, **77**, 094402 (2008).
[16] J. M. Rondinelli and N. A. Spaldin, Phys. Rev. B, **79**, 054409 (2009).
[17] C. Pinta, D. Fuchs, E. Pellegrin, P. Adelmann, S. Mangold, and S. Schuppler, J. Low Temp. Phys., **147**, 421 (2007).
[18] N. Sundaram, Y. Jiang, I. E. Anderson, D. P. Belanger, C. H. Booth, F. Bridges, J. F. Mitchell, T. Proffen, and H. Zheng, Phys. Rev. Lett., **102**, 026401 (2009).
[19] M. W. Haverkort, Z. Hu, J. C. Cezar, T. Burnus, H. Hartmann, M. Reuther, C. Zobel, T. Lorenz, A. Tanaka, N. B. Brookes, H. H. Hsieh, H.-J. Lin, C. T. Chen, and L. H. Tjeng, Phys. Rev. Lett., **97**, 176405 (2006).
[20] C. K. Xie, J. I. Budnick, W. A. Hines, B. O. Wells, and J. C. Woicik, Appl. Phys. Lett., **93**, 182507 (2008).
[21] J. C. Woicik, C. K. Xie, and B. O. Wells, J. Appl. Phys., **109**, 083519 (2011).
[22] S. J. May, J.-W. Kim, J. M. Rondinelli, E. Karapetrova, N. A. Spaldin, A. Bhattacharya, and P. J. Ryan, Phys. Rev. B, **82**, 014110 (2010).
[23] N. M. Souza-Neto, A. Y. Ramos, H. C. N. Tolentino, E. Favre-Nicolin, and L. Ranno, Phys. Rev. B, **70**, 174451 (2004).
[24] P. G. Radaelli and S.-W. Cheong, Phys. Rev. B, **66**, 094408 (2002).
[25] At 1000 K, LCO has a -2.0 % misfit with LAO and a 1.1 % misfit with STO.
[26] J. C. Woicik, B. Ravel, D. A. Fischer, and W. J. Newburgh, J. Synchrotron Rad., **17**, 409 (2010).
[27] EXAFS ($\chi(k)$) is the normalized, background subtracted x-ray absorption. Background subtraction was carried out using the EXAFS data processing program ATHENA; B. Ravel and M. Newville, J. Synchrotron Rad., **12**, 537 (2005).
[28] For further details about fitting with empirical standards see J. C. Woicik and P. Pianetta in *Synchrotron Radiation Research: Advances in Surface and Interface Science*, Vol. 2, editied by R. Z. Bachrach (Plenum Press, New York, 1992) Chap. 6, pp. 211-266; J. C. Woicik, J. A. Gupta, S. P. Watkins, and E. D. Crozier, Appl. Phys. Lett., **73**, 1269 (1998).
[29] Reported error bars represent statistical errors, and give the value of $r_{Co-O}$ that doubles the residual $\chi^2$ from the fit.
[30] J. C. Woicik, E. L. Shirley, C. S. Hellberg, K. E. Andersen, S. Sambasivan, D. A. Fischer, B. D. Chapman, E. A. Stern, P. Ryan, D. L. Ederer, and H. Li, Phys. Rev. B, **75**, 140103 (2007).
[31] G. Vankó, J.-P. Rueff, A. Mattila, Z. Németh, and A. Shukla, Phys. Rev. B, **73**, 024424 (2006).
[32] M. Medarde, C. Dallera, M. Grioni, J. Voigt, A. Podlesnyak, E. Pomjakushina, K. Conder, T. Neisius, O. Tjernberg, and S. N. Barilo, Phys. Rev. B, **73**, 054424 (2006).
[33] G. Vankó, F. M. F. de Groot, S. Huotari, R. J. Cava, T. Lorenz, and M. Reuther, e-print arXiv:0802.2744v1 [cond-mat.str-el] (2008).
[34] C. Brouder, J. Phys.: Condens. Matter, **2**, 701 (1990).
[35] J. Wu and C. Leighton, Phys. Rev. B, **67**, 174408 (2003).
[36] M. A. Señarís Rodríguez and J. B. Goodenough, J. Solid State Chem., **118**, 323 (1995).
[37] C. Pinta, D. Fuchs, M. Merz, M. Wissinger, E. Arac, H. v. Löhneysen, A. Samartsev, P. Nagel, and S. Schuppler, Phys. Rev. B, **78**, 174402 (2008).
[38] M. Merz, P. Nagel, C. Pinta, A. Samartsev, H. v. Löhneysen, M. Wissinger, S. Uebe, A. Assmann, D. Fuchs, and S. Schuppler, Phys. Rev. B, **82**, 174416 (2010).
[39] M. Itoh, I. Natori, S. Kubota, and K. Motoya, J. Magn. Magn. Mater., **140-144**, 1811 (1995).
[40] D. Fuchs, L. Dieterle, E. Arac, R. Eder, P. Adelmann, V. Eyert, T. Kopp, R. Schneider, D. Gerthsen, and H. v. Löhneysen, Phys. Rev. B, **79**, 024424 (2009).